Polyhedron 53 (2013) 20–25

Contents lists available at SciVerse ScienceDirect

Polyhedron

journal homepage: www.elsevier.com/locate/poly

Synthesis, acid–base and complexing properties with Cu(II), Co(II) and Zn(II) in aqueous solution of a novel 1*H*-benzimidazol-2-ylmethyl diethyl phosphate ligand: Comparison with other 2-substituted benzimidazole ligands

Aleksander Kufelnicki [a,*], Magdalena Woźniczka [a], Urszula Kalinowska-Lis [b], Julia Jezierska [c], Justyn Ochocki [b]

[a] *Department of Physical and Biocoordination Chemistry, Faculty of Pharmacy, Medical University of Łódź, 1 Muszyński Str., 90-151 Łódź, Poland*
[b] *Department of Bioinorganic Chemistry, Faculty of Pharmacy, Medical University of Łódź, 1 Muszyński Str., 90-151 Łódź, Poland*
[c] *Faculty of Chemistry, University of Wrocław, 14 F. Joliot-Curie Str., 50-383 Wrocław, Poland*

ARTICLE INFO

Article history:
Received 13 September 2012
Accepted 5 January 2013
Available online 26 January 2013

Keywords:
2-Substituted benzimidazoles
Divalent metals
Bioinorganic chemistry
pH potentiometry
UV–Vis spectroscopy
EPR spectroscopy

ABSTRACT

1*H*-Benzimidazol-2-ylmethyl diethyl phosphate (2-BimOpe) was synthesized via condensation of phosphorochloridic acid diethyl ester with 2-benzimidazolemethanol in the presence of triethylamine. This phosphate derivative of benzimidazole was chosen because of its expected biological properties, indicated up to now for many other related compounds. The coordinating properties of 2-BimOpe towards Cu(II), Co(II) and Zn(II) in aqueous solution have been studied through a combined application of potentiometric and spectroscopic methods (electronic absorption for Cu(II) and Co(II) as well as EPR spectroscopy in the case of Cu(II)). It was shown that 2-BimOpe coordinates Cu(II) yielding CuL and CuL_2 species (the CuL_2 complex being confirmed only by EPR). The same measurements have been made with benzimidazole (Bim) and 2-(hydroxymethyl)benzimidazole (2-CH_2OHBim), the latter ligand capable of bidentate {N,O} coordination. Moreover, the potentiometric results for the novel diethyl phosphate derivative of 1*H*-benzimidazol-2-ylmethanol, 2-BimOpe, have been compared with the literature data reported recently for (1*H*-benzimidazol-2-yl-methyl)phosphonate ($Bimp^{2-}$). The difference between complexation abilities of Bim and 2-BimOpe comes evidently from a bulky effect of the estrificated phosphoric groups preventing the benzimidazole fragment to be involved in the consecutive complexation steps. On the other hand the N(3) nitrogen is the most acidic one ($pK_a = 4.04$) in 2-BimOpe among the compounds considered. The release of the N(3)H^+ proton occurs at a relatively low pH for 2-BimOpe, most probably due to the known electron withdrawing effect of the phosphate group.

1. Introduction

It is known that some Cu(II) and also Zn(II) complexes with 2-substituted benzimidazole ligands indicate biological and pharmacological activity [1,2]. Similarly, such properties involve, among others, the cytotoxic [3,4] and antiviral [4] activity of Pt(II) complexes. On the other hand, the benzimidazole moiety alone, also addressed as 1,3-dideazapurine, is structurally related to purine bases. The benzimidazole residue is also a constituent (axial ligand bound through N3 nitrogen) of vitamin B_{12} and other cobalamines. Then, it is not surprising that the biological properties of benzimidazole and related compounds have been and are still studied intensively because of their antiarrythmic, antibacterial, antiviral, antitumor properties and application in treatment of acid-peptic diseases [5–8]. Recently, the phosphonate derivatives have received significant attention as therapeutic or potentially therapeutic agents [9,10]. Moreover, also many phosphate derivatives of benzimidazole, in particular nucleotide analogs, show various biological properties [11].

The title ligand (2-BimOpe) is a diethyl ester of 1*H*-benzimidazol-2-phosphonic acid described up to now only as a ligand in a trans-bis(1*H*-benzimidazol-2-ylmethyl-κN^3 diethyl phosphate)dichloropalladium(II) monohydrate [12] complex and also investigated as involved in solid chloride Cu(II), Co(II) and Zn(II) complexes well soluble in ethanol [13]. In the copper complex recrystallized from ethanol the Cu atoms together with the chloride ions form a characteristic closed cage-like structure with a water molecule inside. As shown by X-ray structure analysis the Co and Zn complexes are isostructural. Their central metal adopts tetrahedral arrangement with two chloride ions and two endocyclic nitrogen atoms in the coordination sphere. The Cu(II) complex proved to be a cytotoxic agent against the A549 lung cancer cell lines and a human colorectal adenocarcinoma cell line (HT29)

---

[*] Corresponding author. Tel.: +48 42 6779204; fax: +48 42 678 83 98.
E-mail address: aleksander.kufelnicki@umed.lodz.pl (A. Kufelnicki).

0277-5387/$ - see front matter © 2013 Elsevier Ltd. All rights reserved.
http://dx.doi.org/10.1016/j.poly.2013.01.006

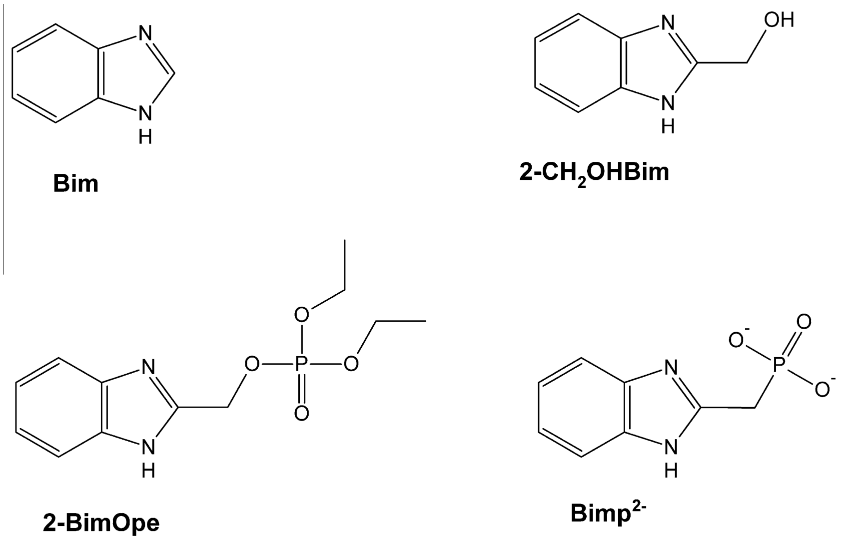

Scheme 1. Structures of the ligands.

[14]. The second active complex was Zn(II) which, in spite of the necessity of being used in high doses, remained virtually neutral for normal human peripheral blood lymphocytes.

The results presented now show the coordination behavior of the synthesized 2-BimOpe in aqueous solution towards three divalent cations (Cu^{2+}, Co^{2+} and Zn^{2+}), which favor rather N than O donors [15]. A comparison is done with benzimidazole (Bim), a ligand coordinating only via the N3 nitrogen and also with two other ligands, 2-(hydroxymethyl)benzimidazole (2-CH_2OHBim) and (1*H*-benzimidazol-2-yl-methyl)phosphonate ($Bimp^{2-}$), which may even participate in chelatation owing to additional O donors in the 2-methyl substituents [10]. To extend the comparison to other metal ions we report here also the attempts of studies on Co(II) complexes with 2-CH_2OHBim.

The structures of the new ligand (2-BimOpe) and these studied as references (Bim, 2-CH_2OHBim as well as $Bimp^{2-}$) are shown in Scheme 1.

2. Experimental

2.1. Materials and physical measurements

Starting materials and solvents for synthesis were obtained commercially and used as received. The silica gel 60 (63–200 mesh, Merck) was used for column chromatography. Analytical thin-layer chromatography was performed using Merck 60 F_{254} silica gel (precoated sheets, 0.2 mm thick). Infrared spectrum was recorded in the range 4000–400 cm^{-1} on a Bruker IFS66 spectrophotometer using KBr pellets. NMR (^1H, ^{31}P) spectra were collected on a Mercury 300 MHz spectrometer using DMSO as a solvent.

2.1.1. Synthesis of 1H-benzimidazol-2-ylmethyl diethyl phosphate (2-BimOpe)

2-Benzimidazolemethanol (0.01 mol, 1.48 g) and triethylamine (0.01 mol, 1.01 g) were dissolved in anhydrous *N*,*N*-dimethylformamide (20 ml) at room temperature. Then diethyl chlorophosphate (0.01 mol, 1.73 g) was added. The reaction mixture was stirred for 1 h at room temperature. The precipitated $N(C_2H_5)_3{\cdot}HCl$ was filtrated and discarded. The solvent (DMF) was evaporated from the solution under reduced pressure by repeated evaporation with toluene. The oily residue was purified by column chromatography (silica gel, acetone) giving a pale yellow oil product: $R_F = 0.54$; $C_{12}H_{17}N_2O_4P$ (M = 284.2 g/mol); (1.59 g, 56% yield). ^1H NMR (300 MHz, DMSO), δ (ppm): 1.22 (t, 6H, $2 \times OCH_2CH_3$); 4.05 (dq, 4H, $2 \times OCH_2CH_3$); 5.18 (d, 2H, (bi)CH_2OP, $^3J_{HP} = 8.1$ Hz); 7.21 (m, 2H, (bi)H(5)H(6)); 7.58 (m, 2H, (bi)H(4)H(7); 12.69 (s, 1H, NH). ^{31}P NMR (121 MHz, DMSO) δ (ppm): −0.375. IR (KBr) νmax (cm^{-1}): (N–H, C–H stretching) 3397(s), 3186(s), 3062(s), 2986(s), 2916(s), (C=N, C=C) 1625(w), 1592(vw), (–CH_2 scissors) 1458(s), 1442(s), (P=O) 1264(vs br), (P–O–C) 1077(s), 1032(vs br), 984(m); (vs: very strong; s: strong; m: medium; w: weak; vw: very weak; br: broad).

2.2. Potentiometric measurements

The stability constants of proton and metal complexes were determined with a Molspin automatic titration kit equipped with a combined microelectrode Russell CMAWL/4/5/S7. All the experiments were carried out at constant temperature of 25.0 ± 0.1 °C. The water soluble ligands were dissolved in 10 ml flasks, filled up with HNO_3 in excess, KNO_3 and in the titrations in presence of the metal also with an appropriate metal nitrate. Then the ionic strength of the final solution was 0.1 (KNO_3). The protonation and formation constants were determined by pH-metric titrations of 4.0 cm^3 samples. Alkali (0.1 M NaOH carbonate-free, Malinckrodt Baker B.V.) was added from a 0.500 cm^3 calibrated micro syringe. The measurement cell was daily calibrated with 0.1 M NaOH in the $-\log[H^+]$ scale by titration of aqueous 0.005 M HNO_3 (containing KNO_3 up to $I = 0.1$), according to the method of Irving et al. [16]. Purified argon was bubbled through the titration vessel to ensure absence of oxygen and carbon dioxide. Overall concentration formation constants: $\beta_{mlh} = [M_mL_lH_h]/[M]^m[L]^l[H]^h$ were calculated from at least three titration files by SUPERQUAD [17] and then HYPERQUAD 2008 [18]. Graphical simulation of speciation diagrams on the basis of calculated constants was carried out by HySS 2009 [19]. The total concentration of the ligand in each sample ranged within $3.0\text{–}5.0 \times 10^{-3}$ M. The metal–ligand interaction was studied at ligand-to-metal ratios 4:1, 6:1 and 8:1. $Cu(NO_3)_2$ p.a. of Fluka, $Co(NO_3)_2$ p.a. of POCh Gliwice and $Zn(NO_3)_2$ p.a. of Fluka were used – the standard solutions were titrated with disodium salt of EDTA in the presence of murexide.

2.3. Spectroscopic measurements

Electronic spectra under argon were recorded on a Cary 50 Bio spectrophotometer, slit width 1.5 nm, equipped with a fiber-optic device. Thanks to this device it was possible to investigate the equilibrium systems spectrophotometrically, simoultaneously with the pH measurements controlled by another Molspin titrator. The fiber-optic probe of 5 mm (which corresponds to path length 1 cm) was dipped directly into the titration vessel (initial volume 25.0 cm^3, total metal concentration 8.3×10^{-4} up to 7.5×10^{-3} M owing to optimum absorbance measurements, ligand:metal ratio 6:1, 8:1, 10:1, temperature 25.0 ± 0.1 °C). In the experiments without the metal the total concentration of L amounted to 1.5–2.0×10^{-4} M. Because of the highly disturbing absorption of the nitrate ion at ca 300 nm, all the UV experiments were carried out mainly in perchlorate medium (electrolyte $NaClO_4$ instead of KNO_3). The ionic strength in aqueous phase was 0.5, i.e. higher than in the solely potentiometric measurements, by that permitting to avoid undesired dilution of samples during titration with 0.1 M NaOH. The used alkali (0.5 M NaOH carbonate-free, Malinckrodt Baker B.V.) was added from a 0.500 cm^3 calibrated micro syringe. After each base addition the pH and EMF were controlled by the Molspin titrator with a combined InLab Semi-Micro (METTLER TOLEDO) electrode. A time delay was given to equilibrate the system. After each point or set of points a pause was made and the spectrum was recorded at a slow scan (300 nm/min). After the collection of each curve, new aliquots of base were added and the procedure repeated. It was therefore possible to collect a spectrum at each titration point or at each chosen pH. The molar absorbances of species have been calculated after deconvolution by HypSpec (part of HYPERQUAD 2008 suite, Protonic Software). The HypSpec program resolves a linear equation system based on Lambert–Beer's law, using the spectrophotometric data and known (or estimated) equilibrium constants, yielding the initial molar absorbances of individual absorbing species. Then, optionally the program can be used to refine the estimated equilibrium constants from spectrophotometric data.

Caution! Perchlorate salts are potentially explosive and were handled only in small quantities with care.

The EPR spectra were measured using a Bruker Elexsys E500 spectrometer equipped with NMR teslameter (ER 036TM) and frequency counter (E 41 FC) at X-band. The simulations of the experimental spectra were performed using computer program WINEPR Simfonia, version 1.26 beta and the program written by Dr. Andrew Ozarowski from NHMFL, University of Florida, with resonance field calculated by diagonalization of energy matrix. The spectra were measured with a modulation frequency 100 kHz, modulation amplitude of 7 gauss and microwave power of 10 mW. The ligand (L) and Cu^{2+} concentrations were $C_L = 5 \times 10^{-3}$ and $C_{Cu2+} = 6.25 \times 10^{-4}$ M, respectively. To avoid the aggregation of Cu(II) complexes in water to the studied solutions 10% (v/v) of ethyl glycol was added.

3. Results and discussion

3.1. Acid–base properties

All the ligands accept a proton at N(3) of the benzimidazole residue. According to Fig. 1 the N(1)H cannot be considered as proton release and coordination site – the end-point in the ligand curve occurs just after adding one equivalent of base needed to neutralize the mineral acid used for protonation. If N(1)H is also a proton release site the number of base equivalents needed to reach the end-point would be relatively higher. Moreover, as it was shown in the literature for related compounds containing the benzimidazole moiety, the N(1)–H site is deprotonated at very high pH 13 [9].

As it follows from Table 1, the N(3) nitrogen is the most acidic ($pK_a = 4.04$) in 2-BimOpe. The release of the accepted $N(3)H^+$ proton occurs at a relatively low pH, most probably due to the known electron withdrawing effect of the phosphate group [20,21]. The solubility of 2-BimOpe at neutral and basic pH is also decreased. Contrariwise, the acidity of $N(3)H^+$ of Bim is only slightly lowered in comparison with two ligands, 2-CH_2OHBim and $Bimp^{2-}$, able to release additional proton and possessing another negative charged group; both these latter ligands are sufficiently soluble in the alkaline medium. Moreover, the acidity constants reported in Table 1 are in reasonable agreement with those of the references cited,

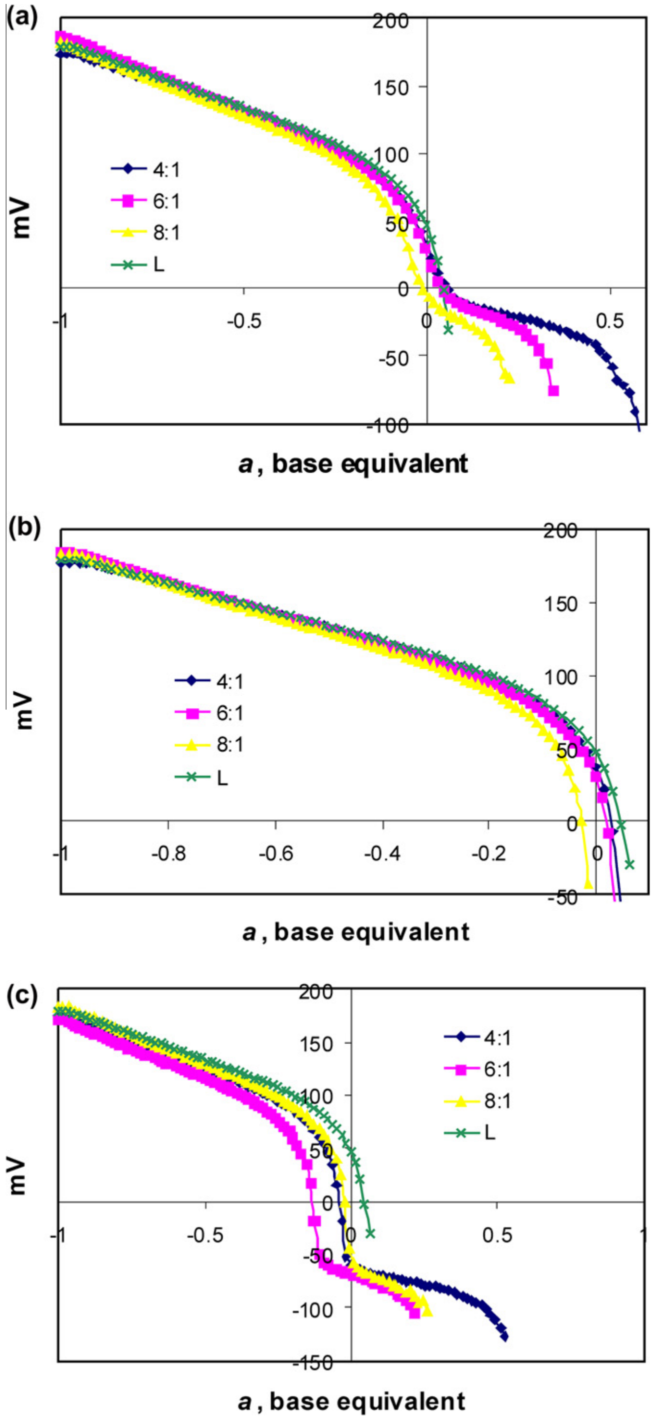

Fig. 1. Titrations of the H^+/Metal ion/2-BimOpe systems under argon. The negative values of base equivalent, *a*, correspond to HNO_3 needed to protonate the ligand. Metal ions: (a) Cu(II), (b) Co(II), (c) Zn(II). Curves: ◆ – ligand-to-metal 4:1, $C_L = 3.0 \times 10^{-3}$ M; ■ – ligand-to-metal 6:1, $C_L = 5.0 \times 10^{-3}$ M; ▲ – ligand-to-metal 8:1, $C_L = 5.0 \times 10^{-3}$ M; × – ligand in absence of the metal, $C_L = 3.0 \times 10^{-3}$ M.

Table 1
Negative logarithms of dissociation constants at 25.0 ± 0.1 °C, $I = 0.1$ (KNO_3) and UV spectral data of the ligands used. Standard deviations in parentheses refer to random errors only. The values are given for the particular sites.

Ligands	$N(3)H^+$		OH		pK_a	Refs.
	pK_a	$\lambda_{max}(\varepsilon_{max})$	pK_a	$\lambda_{max}(\varepsilon_{max})$		
2-BimOpe	4.04(1)		–		–	
		$269(7.9 \times 10^3)$		–		
		$275(7.6 \times 10^3)$				
Bim	5.70(2)		–		5.58	[22]
					5.64	[22]
		$240(3.9 \times 10^3)$			5.54	[23]
		$267(6.2 \times 10^3)$		–	5.68	[24]
		$274(6.7 \times 10^3)$				
2-CH_2OHBim	5.55(6)		11.84(6)		5.40;11.55	[25]
					5.48;11.48	[29]
		$236(4.1 \times 10^3)$		$244(5.8 \times 10^3)$		
		$268(8.5 \times 10^3)$		$273(6.7 \times 10^3)$		
		$275(8.4 \times 10^3)$		$279(8.4 \times 10^3)$		
$Bimp^{2-}$	5.37(2)[a]		7.41(2)[a,b]			[9]

[a] Data found only in [9].

[b] Concerning the $-P(O)_2^-(OH)$ group.

since the differences do not exceed 0.2–0.3 log unit. The analysis of UV absorption spectra via their HypSpec deconvolution on the basis of the equilibrium model accepted potentiometrically (Figs. S1–S3) made possible to determine molar absorbances of the particular ionic species of the ligands – Table 1.

3.2. Complexing behavior

Potentiometric data for 2-BimOpe, although carried out at excess of the ligand (Fig. 1), indicate the formation of L:M = 1:1 species with Cu(II), Co(II) and Zn(II) – Table 2. The complexes exist until pH 7–8 depending on metal ion, whereas in neutral and alkaline solutions the hydrolytic products of the particular cations become the predominant species (example for Cu(II) in Fig. 2). According to Fig. 2, the contribution of metal complex attains maximum relative to the total metal concentration at pH > 4, where more than 50% of the ligand occurs in deprotonated $N(3)H^+$ form. However, the disturbances caused by poorly soluble hydrolytic products at higher pH make impossible to confirm the formation of L:M = 2:1 species, likely owing to the possible next coordination step. Further alkalization leads to appearance and subsequent increasing contribution of the species formed by ML with products of aqua molecules deprotonation. The results for the Zn(II)–2-BimOpe system, based only on potentiometric data owing to the d^{10} configuration of the metal, agree with the results described above for Cu(II) and Co(II) but for two of the three other ligands (Bim and $Bimp^{2-}$) a comparison could be made only with Co(II) (Table 2).

In contrast with Cu(II)–2-BimOpe, the potentiometric results reveal Cu(II) coordination by at least three Bim ligands (Table 2) through N(3), although some literature data indicate that even fourth Bim is bound to Cu(II) [28]. This is possible because a steric hindrance is not produced by this ligand, opposite to 2-BimOpe providing a bulky diethyl phosphate group. Also for the Cu(II)–2-CH_2OHBim system, potentiometric results suggest that more than one N(3) nitrogen donor are involved in the formed complex. Furthermore, the presence of 2-hydroxymethyl O^- donor permits together with N(3) a {N,O} chelatation mode, evidenced in high stability constants (Table 2) by more than six orders of magnitude higher than for solely N(3) coordination.

It seemed to be interesting to compare the potentiometric data of the Cu(II) complexes with the ligands not containing the coordinating oxygen donors beside N(3), with those observed for the complexes with (1*H*-benzimidazol-2-yl-methyl)phosphonate ($Bimp^{2-}$), additionally studied as reference. The first stepwise

Table 2
Logarithms of cumulative stability constants $\beta_{mlh} = [M_mL_lH_h]/[M]^m[L]^l[H]^h$ and UV spectral data [$\lambda_{max}(\varepsilon_{max})$ for Cu^{2+} and Co^{2+}] of the complexes with 2-BimOpe and with the other related ligands at 25.0 ± 0.1 °C, $I = 0.1$ (KNO_3). Standard deviations in parentheses refer to random errors only.

M^{2+}		2-BimOpe	Bim			2-CH_2OHBim		$Bimp^{2-a}$
			Present data	Refs.		Present data	Refs.	
Cu^{2+}	CuL	3.20(3)	3.17(6);	3.44(10);		8.89(4)	9.03;	4.21(8);
	CuL_2		6.15(7);	6.29(3);		16.80(7)	16.81 [29]	7.68(5)
	CuL_3		8.94(8)	8.70(6);	[28a]			
	CuL_4			10.87(9)				
	[$\lambda_{max}(\varepsilon_{max})$]	~440(25)sh 747(30) [d]	312(241)[c] 719(58)[d]			321(530)[c] 717(85)[d]		
Co^{2+}	CoL	3.17(2)	2.74(8)	2.98	[23]	–[b]	–	2.31(8); 4.92(5)
	[$\lambda_{max}(\varepsilon_{max})$]	~440(25)sh 747(30)[d]	510(9)[d]			–[b]	–	
Zn^{2+}	ZnL	3.15(2)	3.00(4)	2.45	[23]	–	–	⩽2.1 5.79(4)

[a] Data found only in [10]. For $Bimp^{2-}$ the two stability constants are stepwise constants, they correspond to the N(3)H and phosphonate protons, respectively.

[b] Measurement disturbance caused by hydrolytic products.

[c] CT transition.

[d] d–d transition.

stability constant of Bimp^{2-} corresponds to coordination via N(3) and is of one order of magnitude higher than the constants for 2-BimOpe and Bim. Apart from the chelate effect the role of negatively charged residue, four bonds away, in facilitating M^{2+} binding at N(3) was shown in Ref. [10].

The wavelengths at maximum and molar absorbances, calculated by deconvolution, are shown in Table 1 (for the ligands) and in Table 2 (for the 2-BimOpe amd Bim complexes with Cu(II) and Co(II) as well as for the Cu(II) complex with 2-CH$_2$OHBim). As it follows, the lower energetic bands species are blue shifted for both the metals relative to the corresponding Cu(H$_2$O)$_6$$^{2+}$ and Co(H$_2$O)$_6$$^{2+}$ aqua ions [26]. Noteworthy is the presence of a weak shoulder at ~440 nm besides the d–d transition of 747 nm usually expected for typical hexacoordinated Cu(II) complexes of distorted octahedral symmetry (Fig. S5). The blue shifts of the asymmetric d–d bands in the visible region, observed for Cu(II) and Co(II) with 2-BimOpe occurred in the pH ranges up to 4.5 for copper(II) and 5.3 for cobalt(II), where the formation of ML reaches maximum (Figs. S4 and S5). Such a result may indicate a slight additional symmetry lowering in relation to the Cu(II) complexes with octahedral geometry distorted by the Jahn–Teller effect, described later in context of Bim and 2-CH$_2$OHBim.

It may be concluded that the electronic absorption spectra could confirm only the first step of complexation both for Cu(II)–Bim and Cu(II)–2-CH$_2$OHBim (Figs. S6 and S7) as alkalization above pH 3.75 or pH 5.0, respectively, brought about a disturbance caused by light scattering arising from the hydrolytic products. A comparison of the spectrophotometric features resulting from titrations and then deconvolution performed by HypSpec (Table 2) shows that the CuL complexes with L = Bim or 2-CH$_2$OHBim are very similar as regarding the coordination modes. Within the visible region, the electronic spectra display absorption at λ_{max} ca 720 nm, whereas in UV range they are characterized by absorption at λ_{max} ca 310–320 nm. This suggests that the remaining coordination sites in Cu(II) centre are occupied by H$_2$O molecules resulting in six-coordinated species. Then, the higher energy bands may be assigned to π–π^* ligand-based LMCT transitions and the lower energy bands to d–d transitions in hexacoordinated Cu(II) complexes with a distorted octahedral geometry [5,26,27].

The spectrophotometric titrations of the systems with Co(II) ions were limited to a very narrow pH range due to the concomitant hydrolysis. A scarce blue shift could be noticed only for Co(II)–Bim within the pH range 4.4–5.5 (Fig. S8) by that indicating only the initial stage of complexation. For Co(II)–2-CH$_3$OHBim the

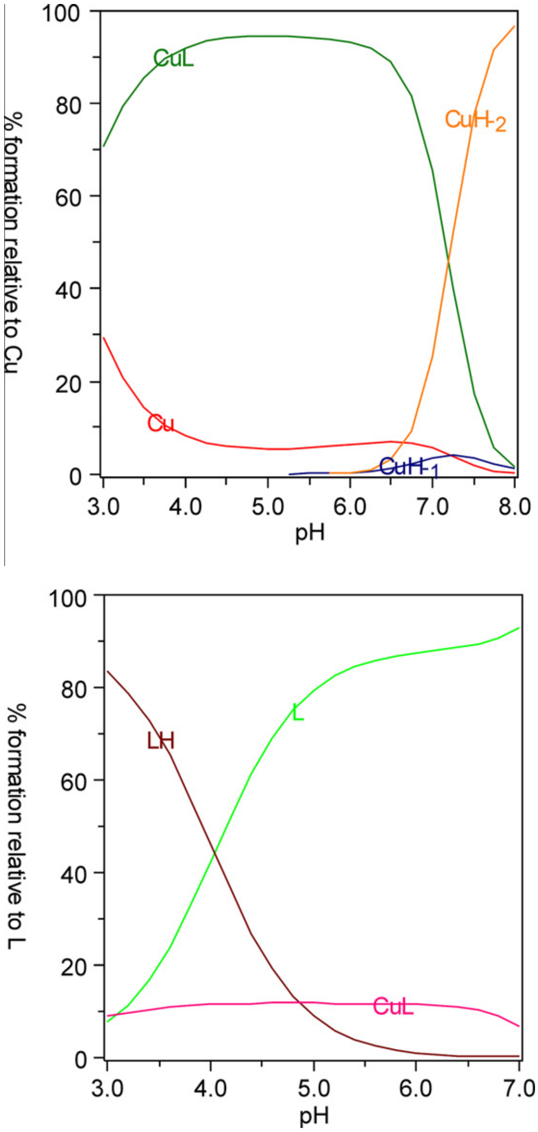

Fig. 2. Species distribution curves as a function of pH for the complexes formed in the Cu(II) ion/2-BimOpe systems at 8:1 ligand-to-metal ratio. $C_L = 5.0 \times 10^{-3}$ M.

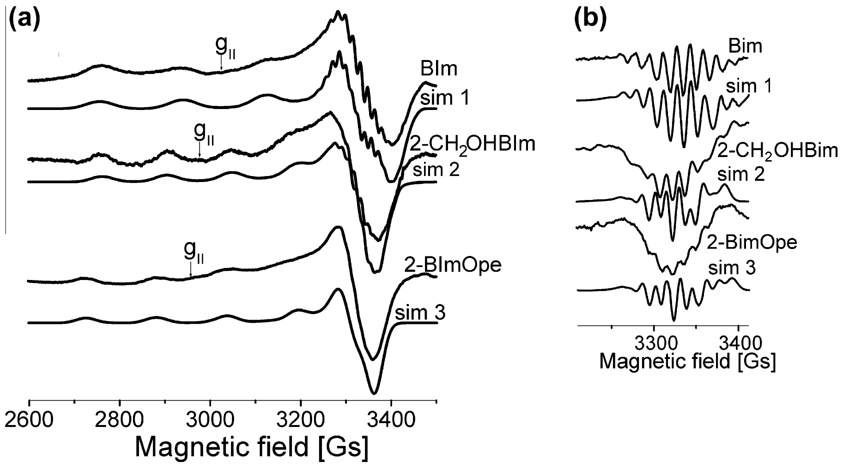

Fig. 3. (a) Frozen solution EPR spectra (single differentiated absorption) of Cu(II) complexes with Bim or CH$_2$OHBim or 2-BimOpe ligands at pH slightly higher than 6, together with simulated spectra (sim1–sim3, respectively) calculated using the parameters given in the Table 3; (b) high-field regions of perpendicular orientation of copper(II) *z* axis to magnetic field direction after next (double) differentiation together with their simulated counterparts (see text).

Table 3
EPR parameters of frozen solutions of Cu(II)–L systems, where L = Bim or 2-CH_2OHBim or 2-BimOpe.

L	pH	$g_{\|}$	$g_{\perp}$	$A_{\|}$ (10^{-4} cm^{-1})	A (^{14}N) [G]
Bim	6.5	2.256	2.054	192	14
2-CH_2OHBim	7.0	2.312	2.062	152	13
2-BimOpe	5.5–6.5	2.312	2.063	169	13

spectrophotometric titrations were disturbed by hydrolytic products already at low pH.

The EPR spectra of the complexes formed in the systems containing Cu(II) ions and ligands: L = Bim or L = 2-CH_2OHBim or L = 2-BimOpe at pH about 6.5 are shown in Fig. 3. The spectra correspond to $g_{\|} \gg g_{\perp} > 2.0023$ relation, typical for axial symmetry of tetragonal geometry of Cu(II) complexes, with $d_{x^2-y^2}$ orbital of unpaired electron being very sensitive to the ligands in *xy* plane. Although 2-BimOpe with the estrificated phosphonic group provides only imidazole nitrogen donor, similarly to that in Bim, the EPR spectra of the formed complexes exhibit higher $g_{\|}$ and lower $A_{\|}$ for the complex with 2-BimOPe ligand (Table 3). It is associated with a smaller amount of the ligands involved in Cu(II) coordination sphere due to bulky effect of estrificated phosphonic groups. The EPR parameters of the complexes formed with 2-CH_2OHBim may be assigned to Cu(II) coordination through two NO chelating ligands supported by the hyperfine splitting pattern assigned to interaction with two nitrogen donors. A second derivative of the resonance absorptions at the magnetic field region close to $g_{\perp}$, exhibited in Fig. 3b, for both the experimental and simulated spectra shows a distinctly resolved splitting due to the hyperfine interaction between Cu(II) unpaired electron and the ligands nitrogen nuclei with $I(^{14}N) = 1$. The best agreement between the hyperfine splitting pattern in experimental and theoretical spectrum was achieved for simulation assuming four nitrogen nuclei for the spectrum of Cu(II)–Bim system and two nitrogen nuclei for the complexes with L = 2-CH_2OHBim and 2-BimOpe. Weak and overlapped EPR spectra of the studied Cu(II) systems at pH about 4.5 show the equilibrium between the Cu(II) ions surrounded by water molecules and the first formed complex with parameters $g_{\|} = 2.360$, $g_{\perp} = 2.070$ and $A_{\|} = 145 \times 10^{-4}$ cm^{-1}, suggesting lower number of nitrogen donors in Cu(II) coordination sphere.

4. Conclusions

The novel 1*H*-Benzimidazol-2-ylmethyl diethyl phosphate N(3)-donor ligand (2-BimOpe) coordinates in the *N*-monodentate mode leading to the monomeric Cu(II), Co(II) and Zn(II) complexes in aqueous solution. Due to the disturbing effects caused by poorly soluble hydrolytic products, the potentiometric and electronic absorption spectroscopy techniques (Cu and Co) confirmed only the first step of complexation. However, the EPR spectroscopy applied to Cu(II) indicated that the second 2-BimOpe ligand is involved in the complexation. At least three nitrogens of bezimidazole (Bim) ligands participating in the coordination sphere of Cu(II) is strongly suggestive that the difference between the complexation abilities of Bim and 2-BimOpe comes evidently from the steric hindrance of the bulky estrificated phosphonic groups. Moreover, a comparison was made for the complexes with 2-(hydroxymethyl)benzimidazole (2-CH_2OHBim) and a recently synthesized (1*H*-benzimidazol-2-yl-methyl)phosphonate ($Bimp^{2-}$), both capable to act as bidentate {N,O} ligands. The non-coordination behavior of the phosphoryl oxygen in 2-BimOpe is probably caused by poor donor properties together with the bulky effect mentioned above. On the other hand, relatively high acidity of the N(3) nitrogen ($pK_a = 4.04$) in 2-BimOpe may be assigned to the known electron withdrawing effect of the phosphate group. Hence, this benzimidazole related ligand may be useful in such biological applications where the metal ion substitutes H^+ ion of the protonated ligand at relatively low pH. It is known, for instance, that the acid–base chemistry of benzimidazole containing proton pump inhibitor is specifically responsible for the acid-catalyzed conversion into the active inhibitors [8].

Acknowledgements

This work was partially supported by the Polish Ministry of Science and Higher Education (Grant No. N405 303236) and by the Medical University of Łódź (Statute Fund No. 503/3-016-02/503-01 – J. Ochocki and Statute Fund No. 503/3-014-02/503-01 – A. Kufelnicki).

Appendix A. Supplementary material

Supplementary data associated with this article can be found, in the online version, at http://dx.doi.org/10.1016/j.poly.2013.01.006.

References

[1] F. Sączewski, E. Dziemidowicz-Borys, P.J. Bednarski, R. Grünert, M. Gdaniec, P. Tabin, J. Inorg. Biochem. 100 (2006) 1389.
[2] J. Wang, L. Shuai, X. Xiao, Y. Zeng, Z. Li, T. Matsumura-Inoue, J. Inorg. Biochem. 99 (2005) 883.
[3] F. Gümüş, Ö. Algül, G. Eren, H. Eroğlu, N. Diril, S. Gür, A. Özkul, Eur. J. Med. Chem. 38 (2003) 473.
[4] M. Gökçe, S. Utku, S. Gür, A. Özkul, F. Gümüş, Eur. J. Med. Chem. 40 (2005) 135.
[5] B. Barszcz, A. Jabłońska-Wawrzycka, K. Stadnicka, J. Jezierska, Polyhedron 27 (2008) 3500.
[6] N.S. Habib, S.M. Rida, E.A.M. Badway, H.T.Y. Fahmy, H.A. Ghozlan, Pharmazie 52 (1997) 346.
[7] S.A.M. El-Hawash, E.A.M. Badaway, T. Kappe, Pharmazie 52 (1999) 341.
[8] (a) M.F. Tutunji, A.M. Qaisi, B. El-Eswed, L.F. Tutunji, Int. J. Pharm. 323 (2006) 110;
(b) A.K. Al-Matar, B. El-Eswed, M.F. Tutunji, Int. J. Chem. Kinet. 41 (2009) 498.
[9] M.J. Sánchez-Moreno, R.B. Gómez-Coca, A. Fernández-Botello, J. Ochocki, A. Kotynski, R. Griesser, H. Sigel, Org. Biomol. Chem. 1 (2003) 1819.
[10] M.J. Sánchez-Moreno, A. Fernández-Botello, R.B. Gómez-Coca, R. Griesser, J. Ochocki, A. Kotynski, J. Niclós-Gutiérrez, V. Moreno, H. Sigel, Inorg. Chem. 43 (2004) 1311.
[11] H. Sigel, L.E. Kapinos, Coord. Chem. Rev. 200–202 (2000) 563.
[12] L. Chęcińska, M. Małecka, J. Ochocki, U. Kalinowska, Acta Crystallogr., Sect E 60 (2004) m1558.
[13] U. Kalinowska-Lis, W.M. Wolf, J. Wojciechowski, J. Ochocki, EUROBIC10, Thessaloniki, Greece, 2010.
[14] R. Kontek, U. Kalinowska-Lis, A. Iwaniuk, J. Ochocki, Italian, Austrian, Czech, Hungarian, Polish, Slovak, Slovenian VII Joint Meeting on Medicinal Chemistry, Catania, Italy, 2011, Book of Abstracts, p. 144.
[15] R.B. Martin, Inorg. Chim. Acta 339 (2002) 27.
[16] H. Irving, M.G. Miles, L.D. Pettit, Anal. Chim. Acta 38 (1967) 475.
[17] P. Gans, A. Sabatini, A. Vacca, J. Chem. Soc., Dalton Trans. (1985) 1195.
[18] P. Gans, A. Sabatini, A. Vacca, Talanta 43 (1996) 1739.
[19] L. Alderighi, P. Gans, A. Ienco, D. Peters, A. Sabatini, A. Vacca, Coord. Chem. Rev. 184 (1999) 311.
[20] T. Kiss, I. Lázár, in: V.P. Kukhar, H.R. Hudson (Eds.), Aminophosphonic and Aminophosphinic Acids. Chemistry and Biological Activity, John Wiley & Sons Ltd., Chichester, 2000, p. 286.
[21] A. Kufelnicki, I. Kupińska, J. Jezierska, J. Ochocki, Pol. J. Chem. 76 (2002) 1559.
[22] X. He, L. Long, X. Le, X. Chen, L. Ji, Z. Zhou, Inorg. Chim. Acta 285 (1999) 326.
[23] G.N. Mukherjee, H.K. Sahu, J. Indian Chem. Soc. 7 (2000) 209.
[24] M.S. Nair, P.T. Arasu, M.A. Neelakantan, Indian J. Chem. 36A (1997) 879.
[25] J.L. Thomas, K.P. Quinlan, J. Am. Chem. Soc. 82 (1960) 2994.
[26] A.B.P. Lever, Inorganic Electronic Spectroscopy, second ed., Elsevier, Amsterdam, 1984. pp. 479, 553.
[27] A.K. Nairn, S.J. Archibald, R. Bhalla, B.C. Gilbert, E.J. MacLean, S.J. Teat, P.H. Walton, J. Chem. Soc., Dalton Trans. (2006) 172.
[28] (a) S. Regupathy, M.S. Nair, Spectrochim. Acta, Part A 75 (2010) 656;
(b) C. Hawkins, D. Perrin, J. Chem. Soc. (1962) 1351 (Resumed).
[29] K. Goverdhan Reddy, K.L. Omprakash, A.V. Chandra Pal, M.L.N. Reddy, Indian J. Chem. 24A (1985) 161.